The relationship between diffusion tensor imaging and volumetry as measures of white matter properties

Anders M. Fjell[*],[a,b], **Lars T. Westlye**[a], **Doug N. Greve**[c], **Bruce Fischl**[c,d], **Thomas Benner**[c], **André J.W. van der Kouwe**[c], **David Salat**[c], **Atle Bjørnerud**[e,f], **Paulina Due-Tønnessen**[g], and **Kristine B. Walhovd**[a,b]

[a]Center for the Study of Human Cognition, Department of Psychology, University of Oslo, Norway

[b]Department of Neuropsychology, Ullevaal University Hospital, Oslo, Norway

[c]Athinoula A. Martinos Center, MGH, Boston, USA

[d]MIT Computer Science and Artificial Intelligence Laboratory, Boston, USA

[e]Department of Medical Physics and the Interventional Centre, Rikshospitalet, University Hospital, Oslo, Norway

[f]Departement of Physics, University of Oslo, Norway

[g]Department of Radiology, Rikshospitalet University Hospital, Oslo, Norway

Abstract

There is still limited knowledge about the relationship between different structural brain parameters, despite huge progress in analysis of neuroimaging data. The aim of the present study was to test the relationship between fractional anisotropy (FA) from diffusion tensor imaging (DTI) and regional white matter (WM) volume. As WM volume has been shown to develop until middle age, the focus was on changes in WM properties in the age range of 40 to 60 years. 100 participants were scanned with magnetic resonance imaging (MRI). Each hemisphere was parcellated into 35 WM regions, and volume, FA, axial, and radial diffusion in each region were calculated. The relationships between age and the regional measures of FA and WM volume were tested, and then FA and WM volume were correlated, corrected for intracranial volume, age, and sex. WM volume was weakly related to age, while FA correlated negatively with age in 26 of 70 regions, caused by a mix of reduced axial and increased radial diffusion with age. 23 relationships between FA and WM volume were found, with seven being positive and sixteen negative. The positive correlations were mainly caused by increased radial diffusion. It is concluded that FA is more sensitive than volume to changes in WM integrity during middle age, and that FA-age correlations probably are related to reduced amount of myelin with increasing age. Further, FA and WM volume are moderately to weakly related and to a large extent sensitive to different characteristics of WM integrity.

Introduction

Integrity of the brain's white matter (WM) is postulated to be significant for cognitive function in both health and disease (Cardenas et al., 2005; Charlton et al., 2006, in press; Choi et al., 2005; Grieve et al., 2007; Tuch et al., 2005; Walhovd and Fjell, 2007). WM change is also a crucial factor in brain aging (Abe et al., 2008; Allen et al., 2005; Bartzokis et al., 2004;

*Corresponding author. Department of Psychology, Pb. 1094 Blindern, 0317 Oslo, Norway. Fax: +47 22 84 50 01. andersmf@psykologi.uio.no (A.M. Fjell).

Kochunov et al., 2007a,[b]; Salat et al., 2005a,b; Walhovd et al., 2005a; Wozniak and Lim, 2006). WM consists largely of myelinated long distance axonal projections of neurons (see below), and is important for integration between brain areas. Using structural magnetic resonance imaging (MRI) it is possible to quantify cerebral WM volume. In addition, diffusion tensor imaging (DTI) can be used to obtain information about the microstructure of WM. Since the diffusion will be stronger parallel with, rather than perpendicular to, myelinated nerve fibers, DTI can be used to gain information about the integrity of nerve fibers. The fractional anisotropy (FA) index is a frequently used metric that expresses the proportion of principal or axial diffusion to radial diffusion, that is, how strongly directional the water diffusion is within a given voxel (Smith et al., 2006). However, a vital question in the understanding and application of DTI and WM volumetry is how they relate to each other. Both are interpreted as measures of WM tissue integrity (Salat et al., 2005b), but little is known about the relationship between them.

The principal aim of the present article is to investigate regional FA and WM volume relations. A large sample of healthy participants between 40 and 60 years was chosen, since cross-sectional MR-studies have indicated that volumetric increase of WM stops sometime around this age range (Allen et al., 2005; Bartzokis et al., 2003; Walhovd et al., 2005a), e.g. at about 45 years (Walhovd et al., 2005a). Insights into microstructural changes associated with this turning point in WM development may contribute to understanding of age-related changes in WM. A newly developed algorithm was used, parcellating WM into 35 different areas in each hemisphere. This procedure was applied for both volumetric estimates and calculation of FA values, thus alleviating the problem of spurious effects due to inaccurate inter-subject registration of DTI volumes and anatomical brain differences (see below). The results of this approach were also compared to the results of a tract-based method described below.

There is reason to expect a relationship between FA and WM volume. FA is related to several aspects of the microstructure of WM, some of which are likely to also affect volume, e.g. degree of myelination and axonal degeneration (Wozniak and Lim, 2006). Both FA (Cascio et al., 2007; Klingberg et al., 1999; Schmithorst et al., 2002; Snook et al., 2007) and WM volume (Courchesne et al., 2000; Giedd, 2004; Giedd et al., 1999, 1996; Pfefferbaum et al., 1994; Wozniak and Lim, 2006) increase in childhood and adolescence, and one underlying factor may be amount of myelin. A similar pattern is seen in the other part of the life-span: WM volume (Allen et al., 2005; Bartzokis et al., 2004; Courchesne et al., 2000; Fotenos et al., 2005; Guttmann et al., 1998; Walhovd et al., 2005a) and FA are then negatively correlated with age (Head et al., 2004; Hugenschmidt et al., 2008; Salat et al., 2005a,b), although the non-linear trajectory often observed for volume has not been reported for FA (Salat et al., 2005b). Age changes in WM tissue in monkeys, e.g. loss of small myelinated fibers and demyelination (Peters et al., 2000), likely affect both WM volume and FA (Hugenschmidt et al., 2008). Postmortem studies have confirmed WM loss (Piguet et al., in press) and myelin breakdown in normal aging (Meier-Ruge et al., 1992; Nielsen and Peters, 2000; Peters et al., 2000; Tang et al., 1997). It is possible that breakdown in tissue integrity, as measured by FA, is an early marker for atrophy that only at a later stage will be detectable by volumetric WM measures. Indirect evidence for myelin state as a possible common factor for WM volume and FA has been reported by Bartzokis and colleagues. After first identifying decline in WM volume with advancing age (Bartzokis et al., 2001), the finding was replicated in a later study by measuring transverse relaxation time, which is assumed to change as a result of myelin breakdown (Bartzokis et al., 2003). This indicates that volumetric changes in aging could be related to myelin breakdown, which likely can be measured by DTI as well.

Still, it must be stressed that FA and volume do not index unitary properties of WM development and aging, but may be sensitive to tissue changes at a number of levels. Even though WM consists of myelinated fibers, they are of different types depending on e.g. the

neurons of origin, of different axon diameters, and are affected by age to different degrees. Axons myelinated later in life often have smaller diameters and seem more vulnerable to age (Bartzokis et al., 2004; Marner et al., 2003; Tang et al.,1997). Further, a large part of WM consists of glial cells, i.e. oligodendrocytes and astrocytes, which may be differentially affected by age (Hayakawa et al., 2007). Thus, many features of WM are not directly related to myelin, and may affect FA and WM volume in different ways. FA reflects aspects of axonal integrity and organization that are not related to myelin (Beaulieu, 2002; Neil et al., 2002; Wozniak and Lim, 2006), and myelin is not necessary for fibers to have significant diffusion anisotropy (Beaulieu and Allen, 1994; Prayer et al., 1997; Wimberger et al., 1995; Wozniak and Lim, 2006). For instance, a packed arrangement of non-myelinated axons may be sufficient to hinder perpendicular water diffusion and thus create anisotropy (Beaulieu and Allen, 1994). Mori and Zhang noted that increased FA in development could be due to myelination, increased axon density, or axonal caliber (Mori and Zhang, 2006). A simple relationship between degeneration of myelin and WM atrophy in aging has not been definitively established (Peters et al., 2000; Peters and Sethares, 2002). Among complicating factors are redundant myelination, sometimes observed with higher age (Peters et al., 2000), which may have different effects on FA and WM volume. The same may be true for fluid bubbles in the myelin sheet, which also have been observed with age (Peters and Sethares, 2002). Finally, FA likely reflects partly different brain characteristics during different phases of development (Wozniak and Lim, 2006) and aging, so that the relationship between FA and WM volume may change during the life-span. In sum, even though a positive correlation between FA and WM volume is expected, there are many factors that may diminish or even reverse this relationship.

So far, only a handful of studies have tested relationships between WM volume and FA. Prefrontal FA has been found to correlate with prefrontal WM volume, but only in participants above 40 years of age (Salat et al., 2005b). In a recent study, correlations between FA and combined voxel-based morphometry were found in several WM areas, including corpus callosum (for length), temporal and parietal regions of the corona radiata, and centrum semiovale (Hugenschmidt et al., 2008). It was suggested that FA reductions precede WM atrophy in parts of the brain. In another study, it was found that FA was negatively related to age, while total WM volume did not correlate with age (Abe et al., 2008). It was concluded that diffusion properties and brain volume are complementary markers of brain aging.

Looking at axial and radial diffusion in addition to FA may yield additional information about WM microstructure. Studying shiverer mice with incomplete myelination but normal axons, Song et al. (2002) found increased radial but not changed axial diffusion. Further, Song et al. (2003) found that axial diffusivity was sensitive to axonal degeneration in mice, and later demyelination was associated with increased radial diffusivity. In a more recent experiment, the same group demonstrated that radial diffusivity was sensitive to both demyelination and re-myelination (Song et al., 2005). Still, Song et al. (2002) found that near complete lack of myelin resulted only in a 20% increase in radial diffusion, demonstrating that factors other than myelin contribute significantly to DTI measures (Wozniak and Lim, 2006). Further, Concha et al. (2006) demonstrated that axial diffusion follows a bi-phasic pattern after injury, where short term increase in diffusion is followed by decrease after longer time periods. This causes problems for the interpretability of axial diffusion parameters, because at the time point of scanning, nearby fibers may be in different phases of axial increase or decrease after minor injuries.

The main aim of the present paper was to investigate the differential relationships between age and regional WM volume and FA, and between these two measures of WM properties in themselves in middle-age. Our main hypothesis was that there is a positive correlation between regional WM volume and regional FA. However, this hypothesis must be regarded as tentative, since there are very few published reports addressing these questions. Further, since the age

range of 40 to 60 years represents a turning point in the development of WM volume, it was expected that WM volume would be relatively insensitive to age. FA, on the other hand, has been found to be linearly related to age, and thus it was expected that negative correlations between FA and age would be found. In addition to FA, axial and radial diffusion were also related to age and WM volume.

Materials and methods

Sample

The sample was drawn from a large longitudinal research project in Oslo, called Cognition and Plasticity through the Life-Span. The study was approved by the Regional Ethical Committee of South Norway (REK-Sør), and written informed consent was obtained from all participants prior to the examinations. Volunteers were recruited by newspaper advertisements. Participants were required to be right handed native Norwegian speakers in the age range 40 to 60 years, feel healthy, not use medicines known to affect central nervous system (CNS) functioning, including psychoactive drugs, not be under psychiatric treatment, be free from worries regarding their memory abilities, and not have injury or diseases known to affect CNS function, including neurological or psychiatric illness, serious head injury, or history of stroke. 105 participants satisfied these criteria. Four participants were excluded due to lack of MRI data. All MR scans were subjected to a radiological evaluation by a specialist in neuroradiology, and the participants were required to be deemed free of significant injuries or conditions. This led to the exclusion of one additional participant, reducing the n to 100. For these (58 F/42 M), mean age was 51.7 years (40–60 years, SD = 4.9). All scored < 16 on Beck Depression Inventory (Beck, 1987) and 27 on Mini Mental State Examination (MMSE) (Folstein et al., 1975). Mean full-scale IQ as measured by Wechsler Abbreviated Scale of Intelligence (Wechsler, 1999) was 113.4 (96–128, SD = 7.2).

MR acquisition

Imaging data were collected using a 12 channel head coil on a 1.5-Tesla Siemens Avanto scanner (Siemens Medical Solutions, Erlangen, Germany). The pulse sequence used for diffusion weighted imaging was a single-shot twice-refocused spin echo-EPI pulse sequence with 30 diffusion gradient directions and the following parameters: repetition time (TR)/echo time (TE) = 8200 ms/82 ms, b-value = 700s/mm^2, pixel size = $2.0 \times 2.0 \times 2.0$ mm. This sequence is optimized to minimize eddy current-induced image distortions (Reese et al., 2003). The sequence was repeated in two successive runs with 10 nondiffusion-weighted images in addition to 30 diffusion weighted images collected per acquisition. Each volume consisted of 64 axial slices. Total scanning time was 11 min, 21s.

The pulse sequences used for morphometric analysis were: two 3D T1-weighted Magnetization Prepared Rapid Gradient Echo (MP-RAGE), with the following parameters: TR/TE/TI/FA = 2400 ms/3.61 ms/1000 ms/8°, matrix 192×192, field of view = 240. Each of the two scans took 7min, 42 s. Each volume consisted of 160 sagittal slices with voxel sizes $1.25 \times 1.25 \times 1.20$ mm. The two MP-RAGEs were averaged to increase the signal-to-noise-ratio.

Morphometric analysis

Regional WM volume was calculated using FreeSurfer (http://surfer.nmr.mgh.harvard.edu/fswiki). The WM parcellation depends on the preceding cortical parcellation (Dale et al., 1999; Dale and Sereno,1993; Fischl and Dale, 2000; Fischl et al., 2001,1999a,b; Segonne et al., 2004, 2005). Briefly, the following procedure was used: A representation of the gray/white matter boundary was reconstructed (Dale et al., 1999; Dale and Sereno, 1993), using both intensity and continuity information from the entire 3D MR volume in the segmentation and deformation procedures. Maps were created using spatial

intensity gradients across tissue classes, and were therefore not simply reliant on absolute signal intensity. Next, by use of an automated labeling system (Desikan et al., 2006; Fischl et al., 2004), the cortex was divided into 33 different gyral-based areas in each hemisphere, as shown in Fig. 1. Mean intra class correlation between this method and manual labeling has been reported to be .84 across all 66 areas, with a mean distance error of less than 1 mm (Desikan et al., 2006). All labels were manually inspected for accuracy. With the exception of the anterior cingulate, the labeling gave accurate results. However, for some of the scans, non cortical areas (medial wall, corpus callosum) extended a bit into the anterior cingulate. Examples of such parcellations are given in Supplementary Fig. 1. Thus, the volume estimation of the anterior cingulate labels was not very accurate for this subset of scans. Analyses for these labels were re-run with the non-optimally parcellated scans excluded.

Based on this cortical parcellation, a newly developed algorithm was used to calculate the WM volume in the gyrus underneath each cortical label. Each WM voxel within a gyrus was labeled according to the label of the nearest cortical voxel. Deep WM was not assigned to a particular cortical area, with a 5mm distance limit. This yielded 33 WM areas in each hemisphere, corresponding to the 33 cortical areas, as shown in Fig. 2. In addition, we obtained the volume of deep WM, which consists of all WM voxels not assigned a cortical label, as well as corpus callosum. The volume of each region was obtained by counting the number of $1mm^3$ voxels included (all scans were re-sampled to 1mm isotropic voxels during the first FreeSurfer processing step).

Estimated intracranial volume (ICV) was used to correct the volumetric data. This was calculated by use of an atlas normalization procedure described by Buckner and colleagues (Buckner et al., 2004). The atlas scaling factor is used as a proxy for ICV, shown to correlate .93 with manually derived ICV (Buckner et al., 2004).

DTI analysis

DTI analyses were done with FreeSurfer. The preprocessing of the 30 direction balanced-echo diffusion data involve motion and eddy-current correction, and averaging across the two continuous runs. Each DW image is registered to the T2-weighted low-*b* ($b = 0$) image (i.e. the image with no diffusion encoding). This registration is a 12 parameter affine one, and accounts for both motion between scans, and for residual eddy-current distortions present in the diffusion weighted images. Note that for the balanced echo sequences the eddy current distortions are small, and in our experience the 12 parameter transforms are sufficient to remove the remaining warping. Finally, a rigid transform is computed that maximizes the mutual information between the T1-weighted anatomical and the T2-weighted low-b image. General linear modeling was used to fit the tensors to the data and create the FA and tensor maps, in addition to three eigenvector and eigenvalue maps. The low-b volume was registered to each subject's anatomical volume, and the FA, eigenvector, and eigenvalue maps were analyzed in register with the low-b. Mean FA, principal/axial (λ_1), and radial (($\lambda_2 + \lambda_3$)/2) diffusion were calculated in each of the 33 gyral WM regions in each hemisphere. To avoid the problem of partial volume effects near the GM/WM border, each label was eroded by one voxel. Only FA values within the remaining WM area were used in the analyses. An example of the eroded mask is given in Fig. 3. The mask lay well inside the WM volume, and the probability of gray matter voxels being included was assumed to be extremely low. Since each participant's FA volume is only registered to the same participant's anatomical volume, the problem of spurious differences in FA due to imperfect inter-participant registration and gross anatomical differences is almost eliminated. In addition to FA, we calculated the axial (principal) and radial diffusion properties. The axial diffusion direction equals the principal diffusion, while the radial equals the mean of the second and third diffusion directions.

Since the DTI analysis strategy used was novel, the analyses were also combined with and compared to an alternative approach. The anatomical T1 volume for each participant was linearly transformed (12 DOF affine registration, cost function: correlation ratio, trilinear interpolation) into MNI152 space by use of FLIRT (Jenkinson and Smith, 2001) from FSL (http://www.fmrib.ox.ac.uk/fsl/index.html), and the subsequent transformation matrix was applied to the FA volume and the FreeSurfer WM parcellations for each participant. Next, masks based on the Mori probabilistic atlas (the JHU white-matter tractography atlas) provided with FSL were created, with a threshold of 5 (of 100). The atlas contains eleven major WM tracts in each hemisphere, which were identified probabilistically by averaging the results of deterministic tractography on 28 normal participants (Hua et al., 2008; Mori et al., 2005; Wakana et al., 2007). The relatively liberal probability threshold was chosen in order to accommodate for inter-subject variation in gross WM fiber architecture. The WM parcellations from FreeSurfer and the different tracts from the Mori atlas were simultaneously used as masks for the FA images. For each FreeSurfer parcellation, the number of voxels that overlapped with each of the eleven Mori tracts was counted. This made it possible to decide which major tracts contributed to each of the FreeSurfer defined WM regions for each participant, and to correlate mean FA from each FreeSurfer WM region with FA from each of the constituting tracts. High positive correlations were expected. These analyses were done for validation purposes, and were thus restricted to one (left, randomly picked) hemisphere only to save space. In addition, mean FA in each of the tracts, not restricted to the overlap with the FreeSurfer WM areas, was calculated. This information was used to test whether use of FreeSurfer WM areas to restrict the FA calculation of the tracts would change the relationship between FA and age. 3D slicer (http://www.slicer.org/) was used to create three dimensional renderings of the probabilistically defined tracts. These tracts were projected onto a semi-transparent template brain ("fsaverage" distributed with FreeSurfer). The FreeSurfer WM parcellations were also projected onto this brain, as well as the result of the FreeSurfer whole-brain segmentation (Fischl et al., 2002). This way, it was possible to visually inspect the anatomical locations of the tracts used, and also the overlap with the FreeSurfer WM parcellations. The three-dimensional renderings are shown in Fig. 4.

Statistics

All analyses were run with statistical outliers excluded. An outlier was defined as an observation for which the studentized deleted residuals exceeded ±2.0. To obtain optimal accuracy, this was done for each correlation separately. First, total and hemispheric gyral WM volume, mean total and hemispheric cortical thickness, and mean and hemispheric gyral WM FA, were correlated with each other and with age. Next, regional WM volume and FA were correlated with age. The correlations were corrected for the influence of sex, and in case of WM volume also ICV. It was also tested whether a non-linear (quadratic) term added significantly to the amount of explained variance. The relationships between FA and WM volume were tested by partial correlations for each label, controlling for age, sex, and ICV. Since the two labels in the anterior cingulate were inaccurate for some of the participants, these correlations were also re-run without these participants. Relationships were investigated further by re-running the correlations with axial and radial diffusion as dependent variables. For comparison purposes, regional FA was also correlated with cortical thickness. Several brain areas that probably correlate with one another were investigated, and Bonferroni corrections for multiple comparisons may thus be too conservative since this approach assumes that the dependent variables are not correlated. Because of this, both uncorrected and corrected p-values (by a factor of 35) were presented.

The results were compared with atlas based tractography in the following manner: First, mean FA in each of the FreeSurfer WM regions was correlated with FA in overlapping tracts, and also with the weighted mean of all tracts included in each WM area. The weighted mean was

obtained by multiplying FA in each tract with the number of voxels overlapping with the given FreeSurfer parcellation, summing these products, and dividing by the total number of overlapping voxels for that area. The weighted mean for each FreeSurfer WM parcellation was then correlated with age and WM volume. T-tests of Fisher's z-transformed correlations were computed to check whether significant differences in the sensitivity to age and/or volume could be detected between the two approaches. In addition, mean FA in each of the eleven tracts was calculated independently of any overlap with the FreeSurfer parcellation. The FA in each of these tracts was correlated with age, and the results compared to the FreeSurfer approach and the combined FreeSurfer – tract-based approach.

Results

Global analyses

Total gyral WM FA correlated −.36 ($p < .001$) with age (sex partialled out), −.28 ($p < .01$) with WM volume (age, sex and ICV partialled out), and .21 ($p < .05$) with cortical thickness (sex and ICV partialled out). When ICV was not partialled out, WM volume and FA did not correlate ($r = −.01$, $p = .95$). When hemispheres were analyzed separately, right and left FA correlated −.26 ($p<.05$) and −.40 ($p<.05$) with age (sex partialled out), respectively. The FA-correlations with right and left WM volume were −.23 ($p < .05$) and −.24 ($p < .05$), and .11 and .06 (n.s.) for right and left cortical thickness (sex, age, and ICV partialled out).

Total gyral WM volume correlated .17 (n.s.) with age, and the hemispheric correlations were .14 and .16 (n.s.) for right and left, respectively (sex and ICV partialled out). For cortical thickness, the age-correlations were −.45 ($p<10^{-5}$) for mean thickness, and −.44 ($p<10^{-5}$) and −.39 ($p<.001$) for right and left hemisphere (sex and ICV partialled out), respectively. After these global analyses, regional analyses were conducted.

Regional analyses: Age effects on WM volume and FA

Mean FA and volume in each parcellated region are presented in Supplementary Table 1. Correlations between age and WM volume, where ICV and sex were controlled for, and between age and FA, where sex was controlled for, are presented in Table 1. Color-coded correlations, projected onto a model of the WM surface, are displayed in Fig. 5. As expected, age and volume were generally weakly related, with ten significant correlations (uncorrected, none survived Bonferroni correction), all positive. When ICV and sex were not regressed out, five correlations were significant, all negative. Follow-up analyses showed that three of the relationships between age and WM volume were best described as non-linear (left posterior cingulate and right and left parietal cortex). The results for these three relationships are presented in Supplementary Table 2.

FA and age were more consistently correlated, and significant negative relationships were identified in 26 regions, five surviving Bonferroni corrections. In no case was a positive correlation significant. Areas with significant correlations were found in frontal (e.g. superior frontal gyrus bilaterally), temporal (e.g. left middle temporal gyrus and temporal pole), and parietal WM (e.g. paracentral gyrus bilaterally), and were often symmetrically distributed across hemispheres. In eight cases significantly better fits were obtained by introducing a quadratic term (lateral occipital and precentral gyrus bilaterally, left paracentral, postcentral, and posterior cingulate gyrus, and right entorhinal WM). These relationships are presented in Supplementary Table 3.

The FA-age correlations were investigated further by studying axial (principal) and radial diffusion, and the results are presented in Table 1. Seven positive correlations between radial diffusion and age were observed in the left hemisphere (one survived Bonferroni correction),

while axial diffusion and age correlated significantly negatively in five cases (one survived Bonferroni correction). In five cases where a negative FA-age correlation was found, neither axial nor radial diffusion were significantly related to age. In the right hemisphere, ten negative correlations between age and axial diffusion were found (three surviving Bonferroni correction), and three positive between age and radial diffusion were observed (none surviving Bonferroni correction). In nine cases where a negative FA-age correlation was found, neither axial nor radial diffusion were significantly related to age.

Relationships between FA and WM volume

Partial correlations between FA and WM volume, where age, sex, and ICV were controlled for, are presented in Table 2. Color coded correlations are displayed in Fig. 5, and scatterplots are shown in Fig. 6. 23 correlations were significant ($p < .05$). This was above what one would expect by chance (three to four correlations should reach $p < .05$ by chance), and eight survived Bonferroni correction. Both positive and negative correlations were identified. In the left hemisphere, positive correlations between FA and WM volume were found in caudal anterior cingulate, cuneus, and entorhinal WM, while negative correlations were found in inferior parietal WM, isthmus of the cingulate, lateral orbitofrontal WM, pars orbitalis, precuneus, rostral anterior cingulate, superior frontal gyrus, and the temporal pole. For the right hemisphere, positive correlations were found in the banks of the superior temporal sulcus, caudal anterior cingulate, cuneus, and rostral middle frontal gyrus, while negative were found in the fusiform gyrus, isthmus of the cingulate, pars orbitalis, postcentral gyrus, precuneus, superior frontal gyrus, superior parietal gyrus, and supramarginal gyrus. Thus, positive correlations that were stable across hemispheres were observed in caudal anterior cingulate WM and cuneus, while symmetric negative correlations were found in isthmus of the cingulate, pars orbitalis, precuneus, and superior frontal gyrus. The correlations for anterior cingulate were re-run with the less accurate parcellations excluded. The positive correlations in left hemisphere in the caudal part (lh: $r = .39$, $p < .05$) survived, while the positive correlation in right hemisphere ($r = .20$, $p < .10$) was only marginally significant. The negative correlations in the left rostral part was now only marginally significant ($r = −.21$, $p < .10$), while the right still correlated weakly ($r = .07$, n.s.).

The correlations were investigated further by correlating WM volume with axial (principal) and radial diffusion, and the results are presented in Table 2. The positive correlations between FA and WM volume were mostly explained by less radial diffusion in the participants with larger WM volumes. In left caudal anterior cingulate, both axial (positive) and radial (negative) diffusion correlated with volume. In cases of negative correlations between FA and volume, positive correlations between radial diffusion and volume were generally found. In four cases (left caudal middle frontal, superior frontal gyrus bilaterally, right supramarginal WM) both axial and radial diffusion were positively related to volume. Generally, radial diffusion was more strongly related to WM volume, with 21 significant correlations across hemispheres (eight positive and thirteen negative), compared to the nine significant correlations between axial diffusion and volume (seven positive, two negative).

Relationships between FA and cortical thickness

For comparison purposes, regional FA was also correlated with cortical thickness, and the results are presented in Table 3. Ten correlations were significant (six in left and four in right hemisphere), of which nine were positive (two survived Bonferroni correction). Bilateral positive correlations were found in the lingual gyrus and precuneus.

Comparison of the WM parcellation and the probabilistic atlas approach

The number of voxels from each of the eleven major WM tracts (see Fig. 4) from the Mori atlas (Hua et al., 2008;Mori et al., 2005;Wakana et al., 2007) was counted for each of the

FreeSurfer WM areas, and the results are presented in Fig. 7. For some WM areas, e.g. the parahippocampal gyrus, only one tract from the Mori atlas contributed (the hippocampal part of the cingulate gyrus), while others included several tracts from the atlas, e.g. isthmus of the cingulate (contributions from the cingulum gyrus, the cingulum-hippocampal gyrus, and forceps major). Typically, each WM area received substantial contributions from two to four tracts although the range was from only one and up to six (and nine for the deep white matter area).

The FA in each part of the tracts that overlapped with the FreeSurfer parcellations was calculated. In addition, a weighted mean of the FA across the contributing tracts within each FreeSurfer WM area was calculated. This was done by multiplying the FA in each tract with the number of voxels overlapping with the FreeSurfer defined WM area, summing the products across tracts in each area, and then dividing by the total number of voxels included. The mean FA of the voxels in each FreeSurfer WM area that was also a part of a Mori tract is presented in Supplementary Table 1. The FAs from the atlas-based tractography approach were generally slightly lower than the FA from the WM parcellation approach alone. The mean difference in FA was .024, which means that the regional tract FA was 5.73% lower than the regional FA based on the FreeSurfer parcellations. Even though the absolute difference in FA between the two approaches was small, an ANOVA with 2 quantification methods (parcellation based, tract based) X FA from 35 WM regions yielded a significant main effect of method (F [1,93] = 693.84, $p < 10^{-44}$). Next, the correlations between FA in the different FreeSurfer areas and FA in each of the contributing tracts were calculated, and these are presented in Table 4. As expected, the correlations were robust and positive. In addition, the mean FA across tracts within each FreeSurfer area was correlated with the FA from that whole area. As expected, robust positive correlations were obtained, and the median correlation reached .82. Thus, the results from the parcellation scheme correlates highly with the results from the atlas-based probabilistic approach.

The sensitivity of each approach to age was compared by checking for significant differences of the correlations obtained by the respective approaches by t-tests of Fishers z-transformed correlation coefficients. The results are presented in Supplementary Table 4. For seven of 35 areas the age-correlation was significantly stronger with the parcellation approach than the tract-based approach. Still, the results from the two approaches were quite similar, in that thirteen and fourteen significant correlations with age was obtained with parcellation-based and the tract-based method, respectively, and for ten regions the correlations were significant with both methods. Finally, FA in each of the eleven tracts was correlated with age without constraining the voxels by the FreeSurfer parcellation scheme. The results are presented in Supplementary Table 5. If no threshold value was used for FA, three significant correlations were found (anterior thalamic radiation $r = -.37$; forceps minor $r = -.27$; uncinate fasciculus $r = -.20$). If only voxels with FA>.20 was used, uncinate fasciculus no longer correlated significantly with age ($r = -.16$, n.s.).

Discussion

Three main conclusions can be drawn from the presented results. First, FA was sensitive to aging even in a relatively narrow age span of 20 years. This was caused by a mix of reduced axial and increased radial diffusion with age. Second, regional WM volume and FA were moderately to weakly related, with correlations going in both directions. FA in the global gyral WM correlated negatively with volume, although this relationship vanished when ICV was not partialled out. Thus, the neurobiological properties underlying individual differences in WM volume and FA are probably somewhat overlapping, but clearly differ to a substantial degree. There were fewer significant correlations between FA and cortical thickness than FA and gyral WM volume, but all except one were in the expected positive direction. Finally, the specific

positive correlations that were identified between FA and WM volume were mainly caused by radial diffusion, suggesting that degree of myelination may contribute to both WM volume and degree of anisotropy in these cases.

Since WM volume is known to stop increasing in middle age, it was expected that the correlation between WM volume and age would be weak. This was confirmed. However, FA correlated with age even within this relatively narrow age range. Thus, age-related changes in WM integrity occur without corresponding observable volumetric reductions. This explanation fits with a view of FA as an early marker for atrophy that at a later stage may be detectable by volumetric WM measures. The FA correlations could partly be explained by increased radial diffusion, suggesting demyelination with increasing age (see below). This is in accordance with results from animal, postmortem studies and MR studies (Bartzokis et al., 2003; Hugenschmidt et al., 2008; Meier-Ruge et al., 1992; Nielsen and Peters, 2000; Peters et al., 2000; Tang et al., 1997) suggesting myelin breakdown with normal aging. Since most cognitive functions depend on distributed neural networks, changes in the myelin integrity will probably affect cognitive function in aging (Bartzokis et al., 2004). This fits with general neuropsychological findings of reduced mental abilities with increasing age, even though the relationship between structural brain changes and cognition is not straightforward (Greenwood, 2007; Raz and Rodrigue, 2006; Raz et al., 2007; Walhovd et al., 2005b). Several of the WM areas where FA and age correlated were frontal (e.g. superior frontal cortex), fitting with the "frontal hypothesis" of aging (West and Bell, 1997; West, 1996), but correlations were found also in several other areas (e.g. inferior parietal and lingual WM).

Regional WM volume and FA were moderately correlated, but to a lesser extent than what was hypothesized. 23 significant correlations are more than expected by chance, but do not indicate a very close relationship. Further, the majority of the correlations were negative, which was contrary to the hypothesis, and the correlation between global gyral WM volume and FA was negative. Of the seven positive correlations, four were symmetrically distributed across the hemispheres (caudal anterior cingulate, cuneus), while eight of the negative correlations were symmetrically distributed (isthmus of the cingulate, pars orbitalis, precuneus, superior frontal gyrus). Even though FA and WM volume are fundamentally different measures, there were several reasons to expect a relationship between the two. Both are negatively affected by age (Head et al., 2004; Hugenschmidt et al., 2008; Salat et al., 2005a,b), even though non-linear age effects on FA are still not established, whereas non-linear age-effects on WM volume have been demonstrated in several cross-sectional studies (e.g. Salat et al., 2005b; Walhovd et al., 2005a,b). Further, both FA and volumetric measures are to some degree related to myelination, at least in mice (Hugenschmidt et al., 2008; Peters et al., 2000; Peters and Sethares, 2002). The latter is in accordance with the present results, in that radial diffusion explained most of the few observed positive relationships.

Several possible explanations may be put forth for why the relationships between FA and WM volume were not stronger. First, FA is probably sensitive to several properties of WM that may not influence volume, e.g. overall variations in brain water content. Further, as argued above, some age-related neurobiological processes have opposite effects on FA and WM volume, e.g. redundant myelination (Peters et al., 2000) and fluid bubbles in the myelin sheets (Peters and Sethares, 2002). Another factor is the complexity of circuitry. Increase in WM volume until middle age may partly be a result of increased complexity of myelinated nerve fibers, with more frequent occurrence of fiber crossing. Increased degree of fiber crossing will reduce the FA index (Tuch et al., 2005), but may contribute to larger WM volume. Myelination of small fibers that are not organized in a parallel fashion will yield low FA, since the voxel size of a typical DTI study is too large to capture the diffusion parallel with the thin fibers. This is a typical property of the WM tissue near the GM/WM border of the brain. The degree of myelination in such areas will affect WM volume and FA in different ways. Thus, it is likely

that a set of different neurobiological processes in sum account for the moderate to weak relationships between WM volume and FA in the present data. It is also interesting to note that the correlations between WM volume and FA generally exceeded the correlations between FA and cortical thickness, but that the latter were positive only.

Studying axial and radial diffusion separately also cast some light on the observed negative correlations between FA and WM volume. For four (left caudal middle frontal, superior frontal gyrus bilaterally, right supramarginal gyrus) of the negative correlations, both axial and radial diffusion correlated positively with volume, indicating increased diffusion in all directions. Further, for twelve of the negative correlations, radial diffusion correlated positively with WM volume. These phenomena can be caused for instance by lower fiber density with more extracellular space. It is possible that such changes will affect diffusion measures and volumetric measures in different ways, although the mechanism behind this is unclear. The positive correlations between radial diffusion and volume may also be caused by increased myelination in areas of substantial fiber crossing. Myelination will probably increase WM volume, but may decrease FA through increased observed radial diffusion because the voxel size is too large to enable disentanglement of small, myelinated crossing fibers. Axon diameter may also influence the radial diffusion, and is an additional candidate explanation for the positive relationship between volume and radial diffusion. The same is degree of fiber packing density, which possibly will affect volume and radial diffusion differently. Beaulieu (Beaulieu, 2002) noted that the non-myelinated olfactory nerve of the garfish has higher anisotropy than the myelinated trigeminal and optical nerves, which may be related to the smaller axonal diameter in the former. However, it must be stressed that the candidate causal relationships discussed here are largely based on speculations, and that more research is needed. Still, studying axial and radial diffusion is probably a fruitful approach in interpreting the microbiological underpinnings for the FA metric.

The present results stand partly in contrast to two previous studies. In one study, correlations between FA and combined voxel-based morphometry (VBM) derived volumes were found in several WM areas (Hugenschmidt et al., 2008). This study had a wide age-range, with 64 participants spanning in age from 18 to 80 years. This probably created more variance in both FA and WM volume than in the present study, thus increasing the probability of identifying significant relationships. Still, the FA-WM correlations were found independently of age, so age-variance per se can probably not explain the divergent results. In another study (Salat et al., 2005b), prefrontal FA and WM volume correlated positively. This correlation was found only when the analysis was restricted to the participants over 40 years. The lack of correlation between FA and WM volume in younger participants was explained by pointing to the typically continued increase in WM volume in this age range in the presence of FA reductions. The age-range in that study, however, was much larger than in the present, extending up to the late seventies. This probably increased the variance in both measures, and age as a common factor for both volume and FA may have added to the likelihood of identifying a relationship. It is possible that WM volume and FA are more strongly correlated in higher age than in middle age. Future research should detail the age trajectories in both WM volume and FA within the same sample.

Comparisons of the parcellation- and tract-based approaches

The purpose of the present paper was not to test approaches to DTI analyses per se, but since the method used is novel, we felt the need for comparing the output of this method with more traditional procedures. The quantification of number of voxels from each of the 11 atlas based tracts in each WM parcellation made it possible to interpret each area in terms of contributing fiber tracts. As expected, areas like superior parietal gyrus and deep WM received contributions from several tracts. All long-projecting fibers in the brain pass though the deep WM, so it was

not surprising that this area received contributions from multiple tracts. The number of tracts included in an area corresponds well to the role of each area in cognitive processing. For instance, the isthmus of the cingulate is an important structure in memory consolidation, as it has connections with medial temporal lobe structures (e.g. hippocampus) and projections forward to the prefrontal cortex (Buckner, 2004). It was therefore expected that this structure would include different fiber tracts. The adjacent posterior cingulate, however, included almost exclusively the cingulum bundle, with a minor contribution from the corticospinal tract. In short, the distribution of tracts within the different parcellations seemed reasonable.

Next, the median correlation of .82 between FA from all the voxels included in a given anatomical WM region and the voxels that were a part of predefined tracts indicated that the parcellation approach yielded comparable results to the more established tract-based method. Further, mean FA in each WM region and the weighted mean of the tracts included in each region was quite similar, with mean differences of about 5%. This difference was highly significant, but the actual difference in mean FA was only .024. The slightly higher FA from the parcellation approach than the tract-based approach may be caused by the relatively low probabilistic threshold that was used for definition of tract. With higher thresholds, the results would probably converge even more.

Finally, when FA from both methods was correlated with an external variable, the results were quite similar. The parcellation approach was slightly more sensitive to age, in that seven of the 35 correlations were higher with this approach. Still, the absolute differences between the coefficients were mostly small, and the low significance levels observed were mainly due to the extremely high correlations between the methods. For instance, the correlations between FA and age in middle temporal WM were −.31 vs. −.21 for the parcellation- vs. the tracts based approach, and this relatively minor difference was significant due to the correlations between FA from the two approaches being as high as .87 for this area. Still, the results were generally similar between the methods. When FA in each tract was calculated without restricting the solutions by the FreeSurfer parcellations, only two tracts correlated significantly with age (anterior thalamic radiation and forceps minor). Thus, FA in gyral WM, whether it was calculated based on the parcellation scheme or the tract-based approach, seemed more sensitive to age than FA in the whole tracts. One reason for this may be that all tracts include a substantial part of the deep WM, which seems to be less influenced by age. This fits with theories of aging of the brain's WM, postulating that later-myelinated fibers, e.g. near the cortex, are more vulnerable to aging than early myelinated fibers (Bartzokis et al., 2004). However, studies employing individual fiber tracking in addition to probabilistic labeling would be an interesting extension of the approach used in the current study.

A major advantage with the parcellation based method is that it facilitates analyses of multi-modal imaging data, in that WM volume and FA is calculated from the same voxels, and both are defined based on the cortical parcellation scheme. Thus, comparisons with cortical variables, such as thickness or volume, can be made. Further, other types of data, e.g. PET metabolism, can be registered to the same volumes and the parcellation scheme can be used for regional analyses of metabolic data.

Limitations

A limitation associated with studies of brain variables in age-homogenous groups, is that the relationships between different variables are treated as static. This may not be an accurate description, however, and FA and WM follow different age-trajectories (Salat et al., 2005b), as also evident from the present data. It has been argued that DTI measures reflect different neurobiological properties of WM at different ages in development (Wozniak and Lim, 2006), and the same is probably true in adult aging as well. Thus, statements about the relationship between brain variables should be restricted to the type of population used in the

study. It is possible that correlations between FA and WM volume will be different in children, middle aged participants, and in elderly. The present results can be regarded as snapshots of a relationship that is in continuous change. The present analyses should be expanded by increasing the age range both upwards and downwards, and by including other groups of participants, e.g. with different types of neurological conditions. This would increase the between-subject variance in the data, and probably the chance of identifying relationships between morphometric and DTI measures. Finally, it is important to keep in mind that even though myelin is an important part of WM, and influences FA to a significant degree, there are other features of WM that also are of importance. Glial cells, i.e. oligodendrocytes and astrocytes, make up a large part of WM.

Conclusions

The present results suggest that regional FA is sensitive to age changes even in a relatively narrow age span of 20 years, at an age where WM volume increases reach a plateau. The reduction of FA with age seems to be partly caused by increased radial diffusion, indicating changes in the integrity of myelin. However, reduced axial diffusion seemed to be as important as increased radial diffusion in explaining age-reductions in FA. Further, WM volume and FA were moderately to weakly correlated. Positive correlations were driven by radial diffusion, presumably related to amount of myelination, while axial diffusion, related to axonal integrity, had relatively less impact on the relationships between FA and volume. Still, at least in healthy, age-homogenous middle aged participants, volume and FA appear sensitive to partly different properties of WM, as evidenced by several negative and non-significant correlations. In conclusion, the results suggest that even though WM volume and FA are to some degree related, great caution should be taken when comparing results from volumetric and FA-studies of WM.

Supplementary Material

Refer to Web version on PubMed Central for supplementary material.

Acknowledgments

Appendix A. Supplementary data

Supplementary data associated with this article can be found, in the online version, at doi: 10.1016/j.neuroimage.2008.06.005.

References

Abe O, Yamasue H, Aoki S, Suga M, Yamada H, Kasai K, Masutani Y, Kato N, Kato N, Ohtomo K. Aging in the CNS: comparison of gray/white matter volume and diffusion tensor data. Neurobiol. Aging 2008;29(1):102–116. [PubMed: 17023094]

Allen JS, Bruss J, Brown CK, Damasio H. Normal neuroanatomical variation due to age: the major lobes and a parcellation of the temporal region. Neurobiol. Aging 2005;26:1245–1260. (discussion 1279–1282). [PubMed: 16046030]

Bartzokis G, Beckson M, Lu PH, Nuechterlein KH, Edwards N, Mintz J. Age-related changes in frontal and temporal lobe volumes in men: a magnetic resonance imaging study. Arch. Gen. Psychiatry 2001;58:461–465. [PubMed: 11343525]

Bartzokis G, Cummings JL, Sultzer D, Henderson VW, Nuechterlein KH, Mintz J. White matter structural integrity in healthy aging adults and patients with Alzheimer disease: a magnetic resonance imaging study. Arch. Neurol 2003;60:393–398. [PubMed: 12633151]

Bartzokis G, Sultzer D, Lu PH, Nuechterlein KH, Mintz J, Cummings JL. Heterogeneous age-related breakdown of white matter structural integrity: implications for cortical "disconnection" in aging and Alzheimer's disease. Neurobiol. Aging 2004;25:843–851. [PubMed: 15212838]

Beaulieu C. The basis of anisotropic water diffusion in the nervous system – a technical review. NMR Biomed 2002;15:435–455. [PubMed: 12489094]

Beaulieu C, Allen PS. Determinants of anisotropic water diffusion in nerves. Magn. Reson. Med 1994;31:394–400. [PubMed: 8208115]

Beck, AaSR. The Psychological Corporation. New York: 1987. Beck Depression Inventory Scoring Manual.

Buckner RL. Memory and executive function in aging and AD: multiple factors that cause decline and reserve factors that compensate. Neuron 2004;44:195–208. [PubMed: 15450170]

Buckner RL, Head D, Parker J, Fotenos AF, Marcus D, Morris JC, Snyder AZ. A unified approach for morphometric and functional data analysis in young, old, and demented adults using automated atlas-based head size normalization: reliability and validation against manual measurement of total intracranial volume. Neuroimage 2004;23:724–738. [PubMed: 15488422]

Cardenas VA, Chao LL, Blumenfeld R, Song E, Meyerhoff DJ, Weiner MW, Studholme C. Using automated morphometry to detect associations between ERP latency and structural brain MRI in normal adults. Hum. Brain Mapp 2005;25:317–327. [PubMed: 15834860]

Cascio CJ, Gerig G, Piven J. Diffusion tensor imaging: application to the study of the developing brain. J. Am. Acad. Child. Adolesc. Psychiatry 2007;46:213–223. [PubMed: 17242625]

Charlton RA, Barrick TR, McIntyre DJ, Shen Y, O'Sullivan M, Howe FA, Clark CA, Morris RG, Markus HS. White matter damage on diffusion tensor imaging correlates with age-related cognitive decline. Neurology 2006;66:217–222. [PubMed: 16434657]

Charlton RA, Landau S, Schiavone F, Barrick TR, Clark CA, Markus HS, Morris RG. A structural equation modeling investigation of age-related variance in executive function and DTI measured white matter damage. Neurobiol. Aging. in press.

Choi SJ, Lim KO, Monteiro I, Reisberg B. Diffusion tensor imaging of frontal white matter microstructure in early Alzheimer's disease: a preliminary study. J. Geriatr. Psychiatry Neurol 2005;18:12–19. [PubMed: 15681623]

Concha L, Gross DW, Wheatley BM, Beaulieu C. Diffusion tensor imaging of time-dependent axonal and myelin degradation after corpus callosotomy in epilepsy patients. Neuroimage 2006;32:1090–1099. [PubMed: 16765064]

Courchesne E, Chisum HJ, Townsend J, Cowles A, Covington J, Egaas B, Harwood M, Hinds S, Press GA. Normal brain development and aging: quantitative analysis at in vivo MR imaging in healthy volunteers. Radiology 2000;216:672–682. [PubMed: 10966694]

Dale AM, Sereno MI. Improved localization of cortical activity by combining EEG and MEG with MRI cortical surface reconstruction: a linear approach. J. Cogn. Neurosci 1993;5:162–176.

Dale AM, Fischl B, Sereno MI. Cortical surface-based analysis. I. Segmentation and surface reconstruction. Neuroimage 1999;9:179–194. [PubMed: 9931268]

Desikan RS, Segonne F, Fischl B, Quinn BT, Dickerson BC, Blacker D, Buckner RL, Dale AM, Maguire RP, Hyman BT, Albert MS, Killiany RJ. An automated labeling system for subdividing the human cerebral cortex on MRI scans into gyral based regions of interest. Neuroimage 2006;31:968–980. [PubMed: 16530430]

Fischl B, Dale AM. Measuring the thickness of the human cerebral cortex from magnetic resonance images. Proc. Natl. Acad. Sci. U. S. A 2000;97:11050–11055. [PubMed: 10984517]

Fischl B, Liu A, Dale AM. Automated manifold surgery: constructing geometrically accurate and topologically correct models of the human cerebral cortex. IEEE Trans. Med. Imaging 2001;20:70–80. [PubMed: 11293693]

Fischl B, Salat DH, Busa E, Albert M, Dieterich M, Haselgrove C, van der Kouwe A, Killiany R, Kennedy D, Klaveness S, Montillo A, Makris N, Rosen B, Dale AM. Whole brain segmentation: automated labeling of neuroanatomical structures in the human brain. Neuron 2002;33:341–355. [PubMed: 11832223]

Fischl B, Sereno MI, Dale AM. Cortical surface-based analysis. II: Inflation, flattening, and a surface-based coordinate system. Neuroimage 1999a;9:195–207. [PubMed: 9931269]

Fischl B, Sereno MI, Tootell RB, Dale AM. High-resolution intersubject averaging and a coordinate system for the cortical surface. Hum. Brain Mapp 1999b;8:272–284. [PubMed: 10619420]

Fischl B, van der Kouwe A, Destrieux C, Halgren E, Segonne F, Salat DH, Busa E, Seidman LJ, Goldstein J, Kennedy D, Caviness V, Makris N, Rosen B, Dale AM. Automatically parcellating the human cerebral cortex. Cereb. Cortex 2004;14:11–22. [PubMed: 14654453]

Folstein MF, Folstein SE, McHugh PR. "Mini-mental state". A practical method for grading the cognitive state of patients for the clinician. J. Psychiatr. Res 1975;12:189–198. [PubMed: 1202204]

Fotenos AF, Snyder AZ, Girton LE, Morris JC, Buckner RL. Normative estimates of cross-sectional and longitudinal brain volume decline in aging and AD. Neurology 2005;64:1032–1039. [PubMed: 15781822]

Giedd JN. Structural magnetic resonance imaging of the adolescent brain. Ann. N. Y. Acad. Sci 2004;1021:77–85. [PubMed: 15251877]

Giedd JN, Blumenthal J, Jeffries NO, Castellanos FX, Liu H, Zijdenbos A, Paus T, Evans AC, Rapoport JL. Brain development during childhood and adolescence: a longitudinal MRI study. Nat. Neurosci 1999;2:861–863. [PubMed: 10491603]

Giedd JN, Rumsey JM, Castellanos FX, Rajapakse JC, Kaysen D, Vaituzis AC, Vauss YC, Hamburger SD, Rapoport JL. A quantitative MRI study of the corpus callosum in children and adolescents. Brain Res. Dev. Brain Res 1996;91:274–280.

Greenwood PM. Functional plasticity in cognitive aging: review and hypothesis. Neuropsychology 2007;21:657–673. [PubMed: 17983277]

Grieve SM, Williams LM, Paul RH, Clark CR, Gordon E. Cognitive aging, executive function, and fractional anisotropy: a diffusion tensor MR imaging study. AJNR Am. J. Neuroradiol 2007;28:226–235. [PubMed: 17296985]

Guttmann CR, Jolesz FA, Kikinis R, Killiany RJ, Moss MB, Sandor T, Albert MS. White matter changes with normal aging. Neurology 1998;50:972–978. [PubMed: 9566381]

Hayakawa N, Kato H, Araki T. Age-related changes of astrocytes, oligodendrocytes and microglia in the mouse hippocampal CA1 sector. Mech. Ageing. Dev 2007;128:311–316. [PubMed: 17350671]

Head D, Buckner RL, Shimony JS, Williams LE, Akbudak E, Conturo TE, McAvoy M, Morris JC, Snyder AZ. Differential vulnerability of anterior white matter in nondemented aging with minimal acceleration in dementia of the Alzheimer type: evidence from diffusion tensor imaging. Cereb. Cortex 2004;14:410–423. [PubMed: 15028645]

Hua K, Zhang J, Wakana S, Jiang H, Li X, Reich DS, Calabresi PA, Pekar JJ, van Zijl PC, Mori S. Tract probability maps in stereotaxic spaces: analyses of white matter anatomy and tract-specific quantification. Neuroimage 2008;39:336–347. [PubMed: 17931890]

Hugenschmidt CE, Peiffer AM, Kraft RA, Casanova R, Deibler AR, Burdette JH, Maldjian JA, Laurienti PJ. Relating imaging indices of white matter integrity and volume in healthy older adults. Cereb. Cortex 2008;18(2):433–442. [PubMed: 17575289]

Jenkinson M, Smith S. A global optimisation method for robust affine registration of brain images. Med. Image. Anal 2001;5:143–156. [PubMed: 11516708]

Klingberg T, Vaidya CJ, Gabrieli JD, Moseley ME, Hedehus M. Myelination and organization of the frontal white matter in children: a diffusion tensor MRI study. Neuroreport 1999;10:2817–2821. [PubMed: 10511446]

Kochunov P, Thompson PM, Coyle TR, Lancaster JL, Kochunov V, Royall D, Mangin JF, Riviere D, Fox PT. Relationship among neuroimaging indices of cerebral health during normal aging. Hum. Brain. Mapp 2007a;29(1):36–45. [PubMed: 17290369]

Kochunov P, Thompson PM, Lancaster JL, Bartzokis G, Smith S, Coyle T, Royall DR, Laird A, Fox PT. Relationship between white matter fractional anisotropy and other indices of cerebral health in normal

aging: tract-based spatial statistics study of aging. Neuroimage 2007b;35:478–487. [PubMed: 17292629]

Marner L, Nyengaard JR, Tang Y, Pakkenberg B. Marked loss of myelinated nerve fibers in the human brain with age. J. Comp. Neurol 2003;462:144–152. [PubMed: 12794739]

Meier-Ruge W, Ulrich J, Bruhlmann M, Meier E. Age-related white matter atrophy in the human brain. Ann. N. Y. Acad. Sci 1992;673:260–269. [PubMed: 1485724]

Mori, S.; Wakana, S.; Nagae-Poetscher, LM.; van Zijl, PCM. MRI Atlas of Human White Matter. Amsterdam: Elsevier; 2005.

Mori S, Zhang J. Principles of diffusion tensor imaging and its applications to basic neuroscience research. Neuron 2006;51:527–539. [PubMed: 16950152]

Neil J, Miller J, Mukherjee P, Huppi PS. Diffusion tensor imaging of normal and injured developing human brain – a technical review. NMR. Biomed 2002;15:543–552. [PubMed: 12489100]

Nielsen K, Peters A. The effects of aging on the frequency of nerve fibers in rhesus monkey striate cortex. Neurobiol Aging 2000;21:621–628. [PubMed: 11016530]

Peters A, Moss MB, Sethares C. Effects of aging on myelinated nerve fibers in monkey primary visual cortex. J. Comp. Neurol 2000;419:364–376. [PubMed: 10723011]

Peters A, Sethares C. Aging and the myelinated fibers in prefrontal cortex and corpus callosum of the monkey. J. Comp. Neurol 2002;442:277–291. [PubMed: 11774342]

Pfefferbaum A, Mathalon DH, Sullivan EV, Rawles JM, Zipursky RB, Lim KO. A quantitative magnetic resonance imaging study of changes in brain morphology from infancy to late adulthood. Arch. Neurol 1994;51:874–887. [PubMed: 8080387]

Piguet O, Double KL, Kril JJ, Harasty J, Macdonald V, McRitchie DA, Halliday GM. White matter loss in healthy ageing: a postmortem analysis. Neurobiol Aging. in press.

Prayer D, Roberts T, Barkovich AJ, Prayer L, Kucharczyk J, Moseley M, Arieff A. Diffusion-weighted MRI of myelination in the rat brain following treatment with gonadal hormones. Neuroradiology 1997;39:320–325. [PubMed: 9189875]

Raz N, Rodrigue KM. Differential aging of the brain: patterns, cognitive correlates and modifiers. Neurosci. Biobehav. Rev 2006;30(6):730–748. [PubMed: 16919333]

Raz N, Rodrigue KM, Haacke EM. Brain aging and its modifiers: insights from in vivo neuromorphometry and susceptibility weighted imaging. Ann. N.Y. Acad. Sci 2007;1097:84–93. % R 10.1196/annals.1379.018. [PubMed: 17413014]

Reese TG, Heid O, Weisskoff RM, Wedeen VJ. Reduction of eddy-current-induced distortion in diffusion MRI using a twice-refocused spin echo. Magn. Reson. Med 2003;49:177–182. [PubMed: 12509835]

Salat DH, Tuch DS, Greve DN, van der Kouwe AJ, Hevelone ND, Zaleta AK, Rosen BR, Fischl B, Corkin S, Rosas HD, Dale AM. Age-related alterations in white matter microstructure measured by diffusion tensor imaging. Neurobiol. Aging 2005a;26:1215–1227. [PubMed: 15917106]

Salat DH, Tuch DS, Hevelone ND, Fischl B, Corkin S, Rosas HD, Dale AM. Age-related changes in prefrontal white matter measured by diffusion tensor imaging. Ann. N. Y. Acad. Sci 2005b;1064:37–49. [PubMed: 16394146]

Schmithorst VJ, Wilke M, Dardzinski BJ, Holland SK. Correlation of white matter diffusivity and anisotropy with age during childhood and adolescence: a cross-sectional diffusion-tensor MR imaging study. Radiology 2002;222:212–218. [PubMed: 11756728]

Segonne F, Dale AM, Busa E, Glessner M, Salat D, Hahn HK, Fischl B. A hybrid approach to the skull stripping problem in MRI. Neuroimage 2004;22:1060–1075. [PubMed: 15219578]

Segonne F, Grimson E, Fischl B. A genetic algorithm for the topology correction of cortical surfaces. Inf. Process. Med. Imaging 2005;19:393–405. [PubMed: 17354712]

Smith SM, Jenkinson M, Johansen-Berg H, Rueckert D, Nichols TE, Mackay CE, Watkins KE, Ciccarelli O, Cader MZ, Matthews PM, Behrens TE. Tract-based spatial statistics: voxelwise analysis of multi-subject diffusion data. Neuroimage 2006;31:1487–1505. [PubMed: 16624579]

Snook L, Plewes C, Beaulieu C. Voxel based versus region of interest analysis in diffusion tensor imaging of neurodevelopment. Neuroimage 2007;34:243–252. [PubMed: 17070704]

Song SK, Sun SW, Ju WK, Lin SJ, Cross AH, Neufeld AH. Diffusion tensor imaging detects and differentiates axon and myelin degeneration in mouse optic nerve after retinal ischemia. Neuroimage 2003;20:1714–1722. [PubMed: 14642481]

Song SK, Sun SW, Ramsbottom MJ, Chang C, Russell J, Cross AH. Dysmyelination revealed through MRI as increased radial (but unchanged axial) diffusion of water. Neuroimage 2002;17:1429–1436. [PubMed: 12414282]

Song SK, Yoshino J, Le TQ, Lin SJ, Sun SW, Cross AH, Armstrong RC. Demyelination increases radial diffusivity in corpus callosum of mouse brain. Neuroimage 2005;26:132–140. [PubMed: 15862213]

Tang Y, Nyengaard JR, Pakkenberg B, Gundersen HJ. Age-induced white matter changes in the human brain: a stereological investigation. Neurobiol. Aging 1997;18:609–615. [PubMed: 9461058]

Tuch DS, Salat DH, Wisco JJ, Zaleta AK, Hevelone ND, Rosas HD. Choice reaction time performance correlates with diffusion anisotropy in white matter pathways supporting visuospatial attention. Proc. Natl. Acad. Sci. U. S. A 2005;102:12212–12217. [PubMed: 16103359]

Wakana S, Caprihan A, Panzenboeck MM, Fallon JH, Perry M, Gollub RL, Hua K, Zhang J, Jiang H, Dubey P, Blitz A, van Zijl P, Mori S. Reproducibility of quantitative tractography methods applied to cerebral white matter. Neuroimage 2007;36:630–644. [PubMed: 17481925]

Walhovd KB, Fjell AM. White matter volume predicts reaction time instability. Neuropsychologia 2007;45:2277–2284. [PubMed: 17428508]

Walhovd KB, Fjell AM, Reinvang I, Lundervold A, Dale AM, Eilertsen DE, Quinn BT, Salat D, Makris N, Fischl B. Effects of age on volumes of cortex, white matter and subcortical structures. Neurobiol. Aging 2005a;26:1261–1270. (discussion 1275–1268). [PubMed: 16005549]

Walhovd KB, Fjell AM, Reinvang I, Lundervold A, Dale AM, Quinn BT, Salat D, Makris N, Fischl B. Neuroanatomical aging: universal but not uniform. Neurobiol. Aging 2005b;26:1279–1283.

Wechsler, D. The Psychological Corporation. San Antonio, TX: 1999. Wechsler Abbreviated Scale of Intelligence.

West R, Bell MA. Stroop color-word interference and electroencephalogram activation: evidence for age-related decline of the anterior attention system. Neuropsychology 1997;11:421–427. [PubMed: 9223146]

West RL. An application of prefrontal cortex function theory to cognitive aging. Psychol. Bull 1996;120:272–292. [PubMed: 8831298]

Wimberger DM, Roberts TP, Barkovich AJ, Prayer LM, Moseley ME, Kucharczyk J. Identification of "premyelination" by diffusion-weighted MRI. J. Comput. Assist. Tomogr 1995;19:28–33. [PubMed: 7529780]

Wozniak JR, Lim KO. Advances in white matter imaging: a review of in vivo magnetic resonance methodologies and their applicability to the study of development and aging. Neurosci. Biobehav. Rev 2006;30:762–774. [PubMed: 16890990]
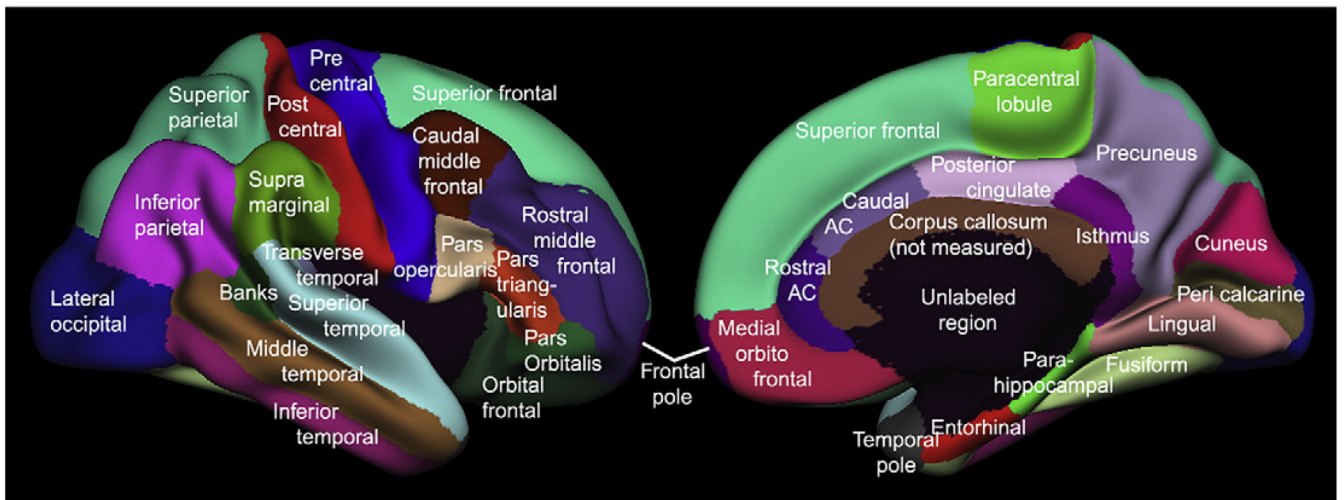
Fig. 1.
Parcellation of the cerebral cortex. The brain surface was parcellated into 33 different gyral based areas, as previously described (Desikan et al., 2006). These areas are shown in different colors on a semi-inflated template brain. The inflation procedure makes it possible to see areas buried inside sulci that would otherwise be hidden from view.
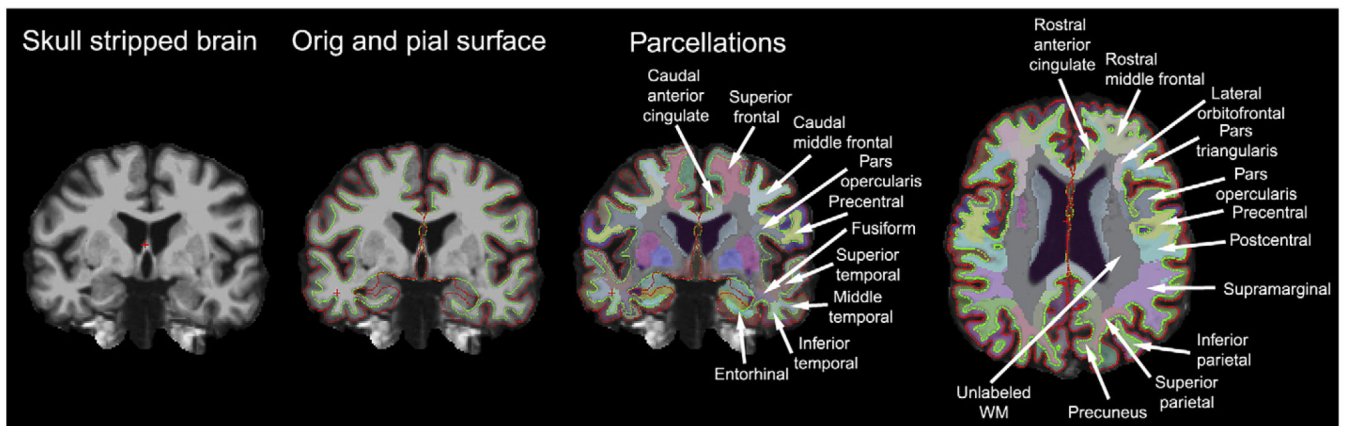
Fig. 2.
Parcellation of the gyral white matter. Gyral white matter was labeled according to the cortical parcellation of the gyri. The image to the left shows the intensity normalized, motion corrected, and skull-stripped mprage scans of a representative participant (58 year old male). In the second image from the left, the gray/white boundaries (orig surface) and the brain/CSF boundaries (pial surface) are illustrated by the red and green line. Examples of the cortical and the WM parcellations are shown in the two right images (coronal and horizontal views, respectively).
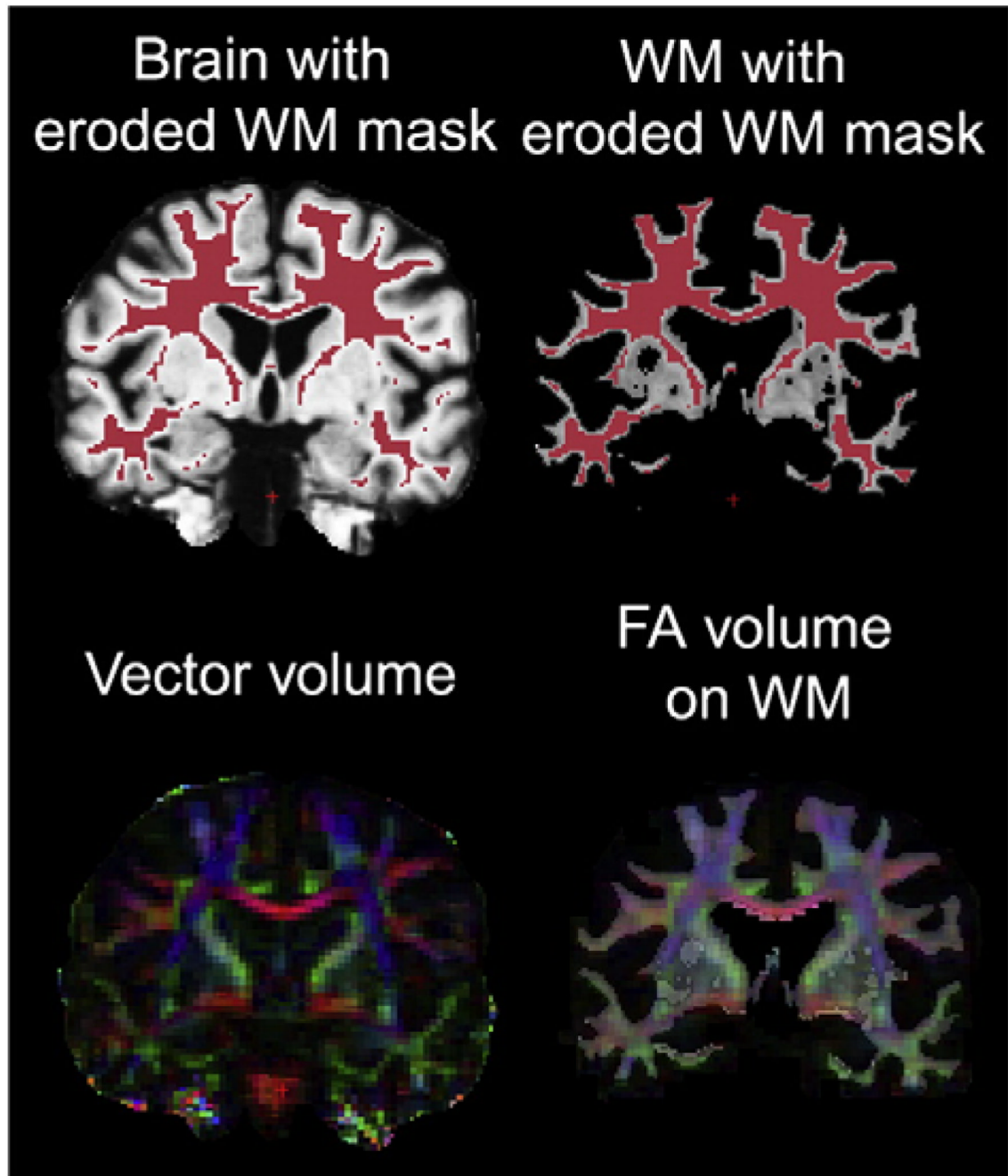
Fig. 3.
Registration of FA to anatomical volumes. The FA images were registered to the anatomical scans, and mean FA in each of the WM parcellations (see Fig. 2) was calculated. Each parcellation was eroded by one voxel, to avoid effects of partial voluming along the cortical/ WM boundary. The upper left image shows the brain volume with the eroded WM mask displayed. The upper right image shows the segmented WM volume with the eroded mask overlaid. As can be seen, the eroded WM mask is embedded well within the WM volume, and the risk of partial voluming is minute. The lower left image is the vector volume registered to the anatomical brain volume, and the lower right image is the transparent vector volume

displayed on the non-eroded WM volume. All images are from the same participant as those in Fig. 2

Anterior thalamic radiation **Cingulum gyrus** **Cingulum gyrus, hippocampal part** **Corticospinal tract**

Forceps major **Forceps minor** **Inferior longitudinal fasciculus** **Inferior occipito-frontal fasciculus**

Superior longitudinal fasciculus **Superior longitudinal fasciculus** **Superior longitudinal fasciculus, temporal part** **Uncinate fasciculus**
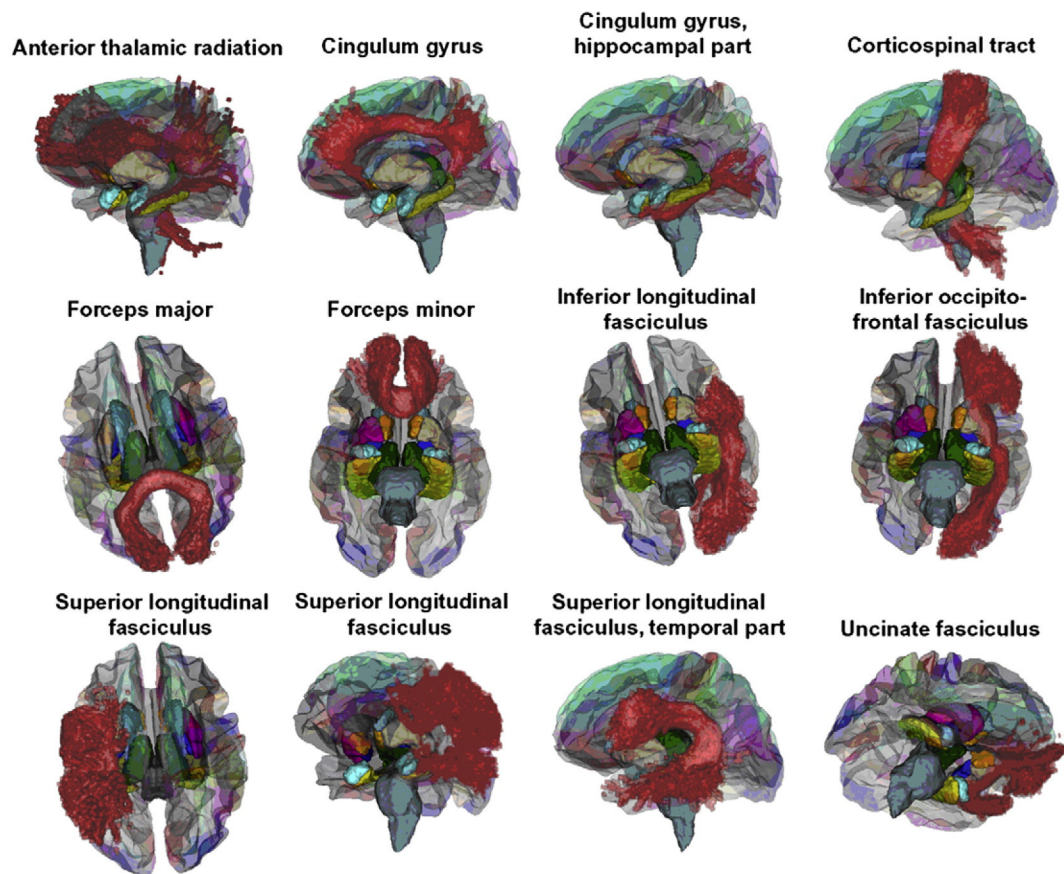
Fig. 4.
3D renderings of the probabilistic tracts overlaid on a transparent template brain with the FreeSurfer WM parcellations and whole-brain segmentation. The 11 atlas-based probabilistic tracts from the Mori atlas is shown as 3D renderings, displayed on a semi-transparent template brain from FreeSurfer (fsaverage). The subcortical structures are results from FreeSurfer's whole brain segmentation procedure. The colors on the cortical surface are the cortical parcellations on which the WM parcellations are based (see Fig. 1 and Fig. 2). The figure was made by use of 3D slicer software (http://www.slicer.org/).
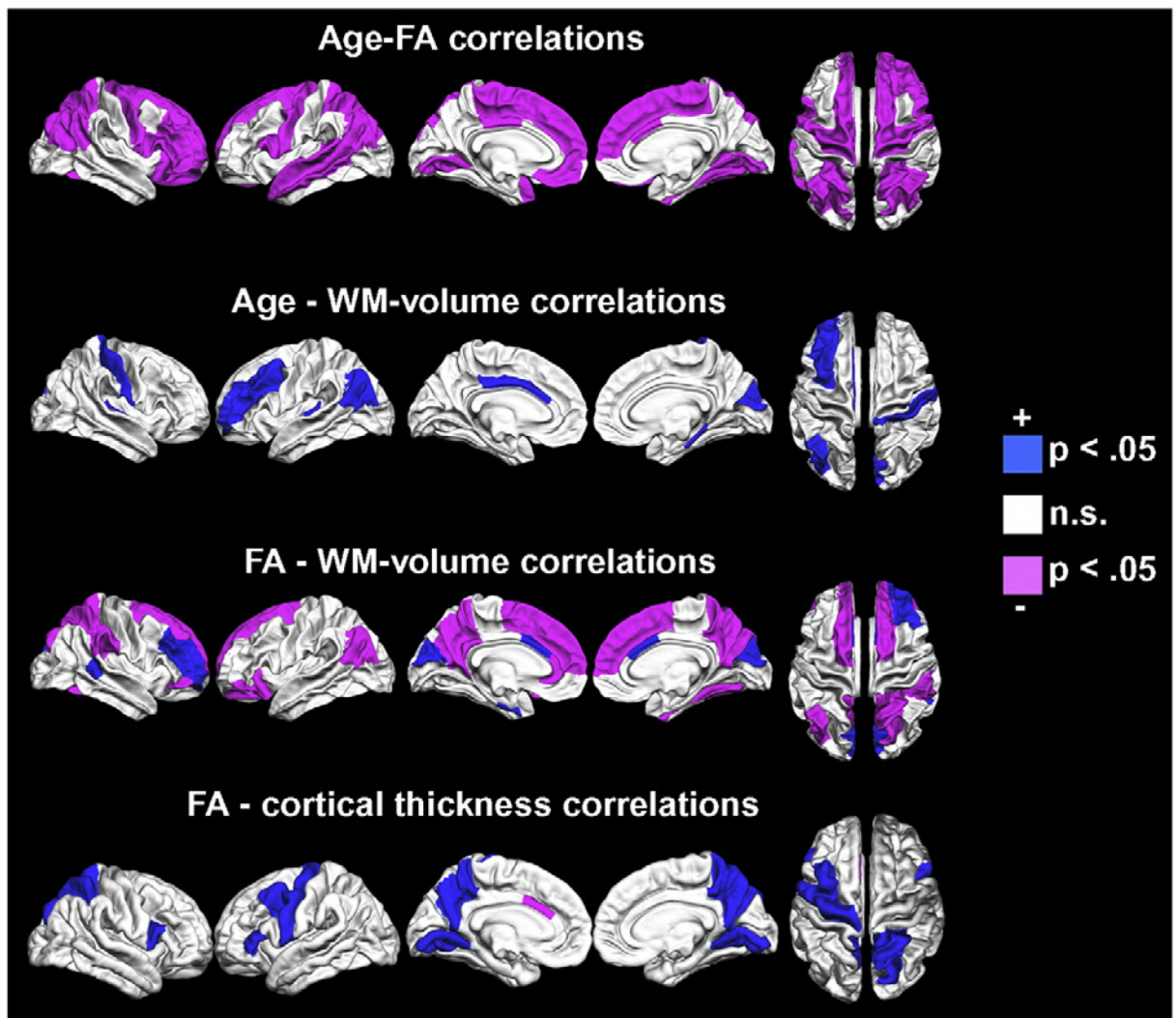
Fig. 5.
Correlations between age, FA, WM volume, and cortical thickness. The significance of the correlations between age and FA (upper panel), age and WM volume (2nd panel), FA and WM volume (3rd panel), and FA and cortical thickness (bottom panel) in each parcellation is color coded, and projected onto a template of the brain's WM (three upper panels) or cortical (bottom panel) surface. The correlations involving WM volume and cortical thickness are corrected for the influence of sex and ICV. The blue color indicate a positive correlation, the pink color indicate a negative correlation.
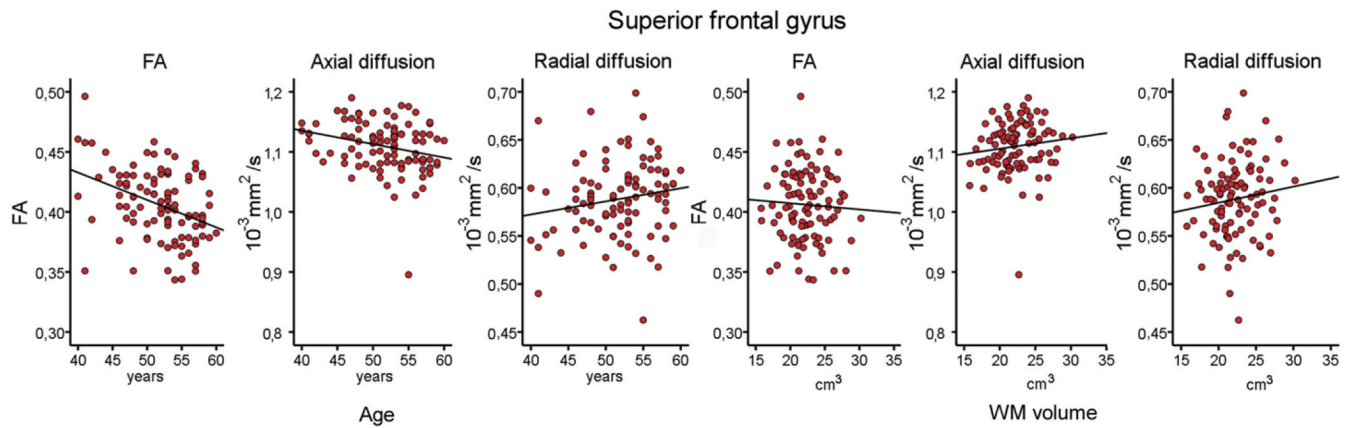
Fig. 6.
Scatterplots of superior frontal gyrus. The figure illustrates the relationship between FA/axial diffusion/radial diffusion and age and WM volume for one selected area (superior frontal gyrus). Note that the scatterplots represent the raw data, while statistics are done with different variables partialled our (age, sex, and/or ICV). In addition, outliers were excluded from all analyses based on a criterion of not exceeding ± 2 studentized deleted residuals, but are included in the scatterplots.
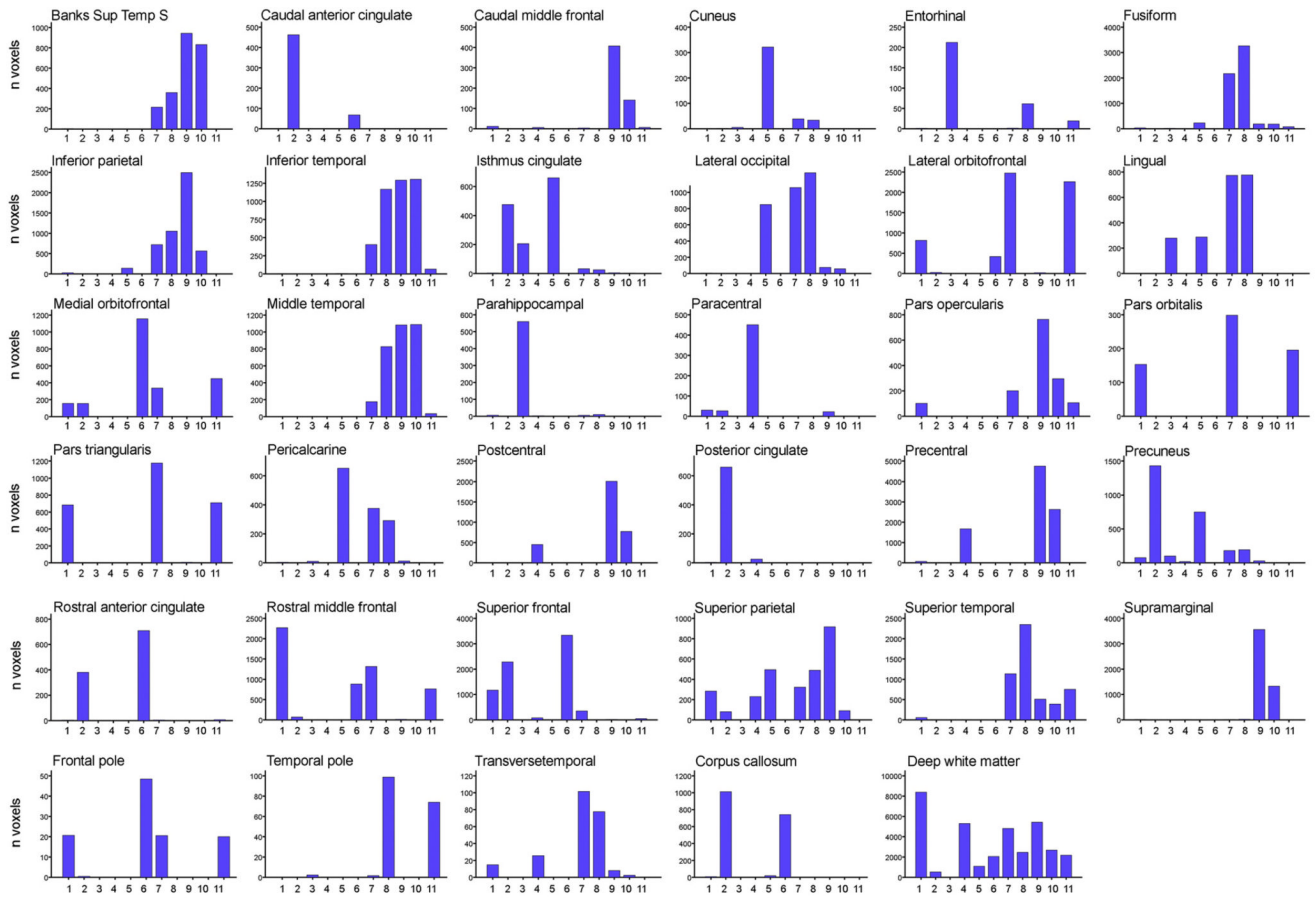
Fig. 7.
Overlap between FreeSurfer parcellations and major tracts from the Mori probabilistic atlas. The bar plots show the number of voxels in each left hemisphere FreeSurfer WM parcel that overlapped with each of the 11 major tracts in the probabilistic atlas used (Mori). Tract numbers refer to 1. ATR, 2. CCG, 3. CHG, 4. CST, 5. FMa, 6. FMi, 7. IFOF, 8. ILF, 9. SLF, 10. SLFTP, 11. UF (see also Fig. 4 and Table 4).

Table 1

Pearson correlations between regional WM volume/DTI and age (outliers are excluded, ±2 studentized deleted residuals)

| WM region	Left hemisphere volume		Right hemisphere volume		Left hemisphere DTI			Right hemisphere DTI		
	r	Partial r[a]	r	Partial r[a]	FA	Axial	Radial	FA	Axial	Radial
Banks Sup Temp S	−.14	.02	−.23	−.14	−.33	−.21	.31	−.03	−.13	.06
Caudal ant cingulate	.13	.23	−.14	−.05	−.09	−.04	.05	−.22	−.14	.19
Caudal middle frontal	.05	.22	−.04	.08	−.18	−.03	.07	−.17	−.17	.07
Corpus callosum	−.08	.02	−.19	−.10	−.10	−.12	.10	−.08	−.09	.05
Cuneus	−.12	.01	.02	.22	−.12	−.10	.07	.00	−.21	−.17
Entorhinal	−.17	−.09	−.07	−.04	−.12	−.10	.09	.05	.06	.10
Fusiform	−.22	−.04	−.06	.18	−.17	−.04	.09	−.20	−.10	.03
Inferior parietal	−.03	.24	−.07	.18	−.27	−.20	.08	−.21	−.11	−.01
Inferior temporal	−.16	−.06	−.16	−.04	−.11	.11	.13	−.02	−.08	−.02
Isthmus cingulate	−.08	−.04	−.05	.09	.07	.01	−.02	−.01	−.02	.01
Lateral occipital	−.15	−.06	−.18	−.06	−.05	−.09	−.07	.03	−.08	−.09
Lateral orbitofrontal	−.13	.08	−.14	.06	−.13	−.02	.14	−.25	−.23	.14
Lingual	−.05	.14	−.11	.06	−.27	−.17	.20	−.27	−.27	.04
Medial orbitofrontal	−.15	.06	−.15	.05	−.29	−.42	.08	−.11	−.21	.05
Middle temporal	−.20	−.03	−.27	−.17	−.31	−.12	.34	−.18	−.20	.22
Parahippocampal	−.02	.14	.02	.25	−.06	−.10	.03	.00	.10	.04
Paracentral	.01	.18	−.02	.16	−.27	−.12	.15	−.26	−.18	.19
Pars opercularis	−.15	.07	.03	.18	−.27	−.13	.25	−.32	−.20	.17
Pars orbitalis	−.12	.02	−.03	.13	−.15	−.04	.04	−.29	−.15	.15
Pars triangularis	−.19	−.09	−.05	.14	−.20	.01	.29	−.26	−.05	.20
Pericalcarine	−.00	.11	−.06	.07	−.11	−.17	.06	−.12	−.33	.01
Postcentral	−.13	.01	−.08	.22	−.14	−.06	.16	−.19	−.07	−.06
Posterior cingulate	.12	.25	−.06	.07	−.24	−.29	.26	−.03	−.08	.09
Precentral	−.02	.19	−.10	.12	−.29	−.12	.12	−.35	−.21	.09
Precuneus	−.17	−.03	−.14	.03	−.12	−.14	.10	−.18	−.33	−.07
Rostral ant cingulate	−.07	.05	.00	.12	−.19	−.04	.13	.04	.08	.01

NIH-PA Author Manuscript

WM region	Left hemisphere volume		Right hemisphere volume		Left hemisphere DTI			Right hemisphere DTI		
	r	Partial r[a]	r	Partial r[a]	FA	Axial	Radial	FA	Axial	Radial
Rostral middle frontal	.02	**.28**	**−.20**	−.10	−.18	−.02	.06	**−.21**	−.17	**.22**
Superior frontal	−.18	−.01	−.11	.11	**−.42**	**−.27**	**.23**	**−.38**	−.14	**.29**
Superior parietal	−.03	.19	−.17	−.04	**−.27**	−.12	.10	**−.30**	−.15	.08
Superior temporal	**−.22**	−.11	−.07	.14	**−.24**	−.12	**.23**	.02	.07	.00
Supramarginal	−.06	.17	−.12	.05	−.17	−.02	.15	−.06	−.05	.05
Frontal pole	.01	.07	−.01	.06	−.09	−.02	.07	−.07	.04	.10
Temporal pole	.08	.20	−.09	.05	**−.23**	.08	.14	−.10	.07	.11
Transverse temporal	.11	**.22**	.07	**.25**	−.11	−.05	.14	−.19	**−.27**	.13
Deep white matter	−.07	.17	−.05	.19	.00	−.12	.01	−.13	−.12	.05

Bold indicates $p \le .05$, $df = 88$–95.

Underlined indicates $p \le .05$ after Bonferroni correction.

[a] Partial correlations corrected for ICV and sex.

Table 2

Partial correlations (controlling for age, sex, and ICV) between regional white matter volume and FA, axial, and radial diffusion (outliers are excluded, ±2 studentized deleted residuals based on each of the relationships between FA/axial diffusion/radial diffusion and white matter volume)

Label	LH correlations with volume			RH correlations with volume		
	FA	Axial	Radial	FA	Axial	Radial
Banks Sup Temp S	.14	−.02	−.16	**.27**	.11	−**.22**
Caudal anterior cingulate	**.37**	−**.24**	−**.24**	**.24**	.17	−**.22**
Caudal middle frontal	−.17	**.30**	**.33**	−.09	.20	.19
Corpus callosum	.11	.13	−.18	.06	.02	−.11
Cuneus	**.28**	.20	−**.29**	**.33**	.06	−**.32**
Entorhinal	**.36**	.05	−**.26**	−.09	−.09	.03
Fusiform	−.09	−.11	.00	−**.22**	−.00	.16
Inferior parietal	−**.31**	.00	**.25**	−.05	.08	.12
Inferior temporal	−.08	−.02	**.14**	.03	−.13	−.13
Isthmus cingulate	−**.28**	.00	**.32**	−**.25**	.16	**.38**
Lateral occipital	.07	−.02	−.09	.14	−.09	−**.21**
Lateral orbitofrontal	−**.39**	.05	**.36**	−.12	.10	.16
Lingual	.05	−.05	−.14	.10	.09	.02
Medial orbitofrontal	.04	.07	.01	−.11	.09	.12
Middle temporal	.13	−.05	−.14	.10	.14	−.08
Parahippocampal	.02	.17	.09	−.10	−.10	.02
Paracentral	.06	.14	.09	−.04	.05	.08
Pars opercularis	−.19	−.16	.14	−.10	.02	.08
Pars orbitalis	−**.22**	.05	.16	−**.22**	−.07	.15
Pars triangularis	.09	−.15	−.12	−.14	−.09	.13
Pericalcarine	.19	**.21**	−.07	.16	.12	−.09
Postcentral	−.13	.02	.05	−**.28**	−.03	.14
Posterior cingulate	.05	**.41**	−.02	.06	**.25**	.03
Precentral	.06	.13	.03	.08	−.10	−.06
Precuneus	−**.34**	−.05	**.25**	−**.24**	−.17	**.23**
Rostral anterior cingulate	−**.24**	−.10	**.22**	.12	.08	−.10

Label	LH correlations with volume			RH correlations with volume		
	FA	**Axial**	**Radial**	**FA**	**Axial**	**Radial**
Rostral middle frontal	.21	−.03	−.18	**.32**	−.05	**−.24**
Superior frontal	**−.32**	**.26**	**.41**	**−.44**	**.26**	**.47**
Superior parietal	−.19	−.01	.14	**−.42**	.08	**.38**
Superior temporal	−.02	−.03	.02	−.12	−.15	.12
Supramarginal	.07	.15	.01	**−.22**	**.28**	**.26**
Frontal pole	−.02	−.12	−.09	.16	−.10	−.13
Temporal pole	**−.25**	−.09	**.21**	−.05	.02	.05
Transverse temporal	−.14	**−.26**	.05	.11	.19	.01
Deep white matter	−.12	.14	**.22**	−.17	.14	**.22**

Bold indicates $p \le .05$, $df = 88–95$.

Underlined indicates $p \le .05$ after Bonferroni correction.

Table 3

Partial correlations (controlling for sex and ICV) between FA and cortical thickness (outliers are excluded, ±2 studentized deleted residuals)

Label	LH	RH
Banks Sup Temp S	.17	−.05
Caudal anterior cingulate	**−.46**	−.20
Caudal middle frontal	**.22**	.00
Cuneus	.20	.19
Entorhinal	−.10	−.03
Fusiform	−.04	.17
Inferior parietal	−.02	.20
Inferior temporal	.09	−.10
Isthmus cingulate	.20	.13
Lateral occipital	.08	.10
Lateral orbitofrontal	.10	.15
Lingual	**.30**	**.44**
Medial orbitofrontal	−.19	−.04
Middle temporal	−.01	.10
Parahippocampal	−.03	.22
Paracentral	.16	.05
Pars opercularis	.06	**.22**
Pars orbitalis	.13	.06
Pars triangularis	**.28**	.08
Pericalcarine	−.00	.19
Postcentral	.20	−.12
Posterior cingulate	.10	−.03
Precentral	**.23**	.08
Precuneus	**.31**	**.26**
Rostral anterior cingulate	.04	−.13
Rostral middle frontal	−.08	−.19
Superior frontal	.03	.05
Superior parietal	.12	**.21**
Superior temporal	.18	−.01
Supramarginal	.07	.05
Frontal pole	.18	−.04
Temporal pole	−.03	.02
Transverse temporal	−.05	.04

Bold indicates $p \leq .05$, $df = 88$–95.

Underlined indicates $p \leq .05$ after Bonferroni correction.

Table 4

Correlations between FA from the FreeSurfer WM parcellations and FA from each of the contributing tracts from the probabilistic atlas (the JHU white-matter tractography atlas, provided with the FMRIB Diffusion Toolbox)

	ATR	CCG	CHG	CST	FMa	Fmi	IFOF	ILF	SLF	SLFTP	UF	Mean
Banks STS							.55	.63	.85	.72		.85
Caudal ant cing		.82				.68						.82
Caudal m frontal		.72							.56	.50		.55
Corpus callosum						.45						.73
Cuneus					.71							.71
Entorhinal								.56				.69
Fusiform							.81	.87				.87
Inferior parietal							.53	.65	.84	.62		.87
Inferior temporal							.47	.78	.66	.65		.77
Isthmus cing		.53	.39		.51		.78	.82				.85
Lat occipital					.65		.78	.82				.84
Lat orbitofront	.39						.63				.59	.69
Lingual			.51		.62		.75	.72				.86
Med orbitofront	.45	.48				.86	.81				.54	.86
Middle temporal								.73	.82	.82		.87
Parahippocampal			.61									.61
Paracentral				.60								.60
Pars opercularis							.58		.76	.54		.79
Pars orbitalis	.64						.76				.73	.78
Pars triangularis	.79						.82				.87	.86
Pericalcarine					.84		.78	.74				.88
Postcentral				.49					.73	.58		.80
Posterior cing		.78										.78
Precentral				.70					.79	.67		.83
Precuneus					.61							.84
Rostral ant cing		.52	.82		.75							.80
Rostral m front	.75					.50	.67				.54	.72
Superior frontal	.46	.56				.51						.72

	ATR	CCG	CHG	CST	FMa	Fmi	IFOF	ILF	SLF	SLFTP	UF	Mean
Superior parietal	.72			.46	.64		.60	.61	.67			.85
Superior temp							.82	.82	.66	.64	.65	.91
Supramarginal									.91	.65		.89
Frontal pole	.05					.69	.52				.48	.61
Temporal pole								.76			.78	.82
Transverse temp							.64	.28				.30
Deep WM	.49			.65	.03	.46	.60	.62	.70	.73	.30	.86

Correlations above .20 were significant. All analyses are done for the left hemisphere only. The median correlation was .82.

ATR: Anterior Thalamic Radiation.

CCG: Cingulum–cingulum gyrus.

CHG: Cingulum–hippocampus gyrus.

CST: Cortico–spinal tract.

FMa: Forceps major.

FMi: Forceps minor.

IFOF: Inferior fronto-occipital fasciculus.

ILF: Inferior longitudinal fasciculus.

SLF: Superior longitudinal fasciculus.

SLFTP: Superior longitudinal fasciculus temporal part.

UF: Uncinate fasciculus.

Mean: The mean FA of all overlapping voxels from the major tracts contributing to each FreeSurfer WM region, weighted by the number of voxels.